



Statistical-dynamical modeling of the cloud-to-ground lightning activity in Portugal



J.F. Sousa ^{a,b,*}, M. Fragoso ^c, S. Mendes ^{d,e}, J. Corte-Real ^d, J.A. Santos ^a

^a Centre for the Research and Technology of Agro-Environmental and Biological Sciences, Physics Department, University of Trás-os-Montes e Alto Douro, Vila Real, Portugal

^b Instituto Português do Mar e da Atmosfera, Lisboa, Portugal

^c Centre for Geographical Studies, Institute of Geography and Spatial Planning, University of Lisbon, Lisbon, Portugal

^d Institute of Mediterranean Agrarian and Environmental Sciences (ICAAM), Group Water, Soil and Climate, University of Évora, Évora, Portugal

^e Geophysical Institute, University of Bergen, Bergen, Norway

ARTICLE INFO

Article history:

Received 7 December 2012

Received in revised form 28 February 2013

Accepted 29 April 2013

Keywords:

Cloud-to-ground discharge
Statistical-dynamical modeling
Lightning regime
Logistic modeling
Lightning forecasting
Portugal

ABSTRACT

The present study employs a dataset of cloud-to-ground discharges over Portugal, collected by the Portuguese lightning detection network in the period of 2003–2009, to identify dynamically coherent lightning regimes in Portugal and to implement a statistical-dynamical modeling of the daily discharges over the country. For this purpose, the high-resolution MERRA reanalysis is used. Three lightning regimes are then identified for Portugal: WREG, WREM and SREG. WREG is a typical cold-core cut-off low. WREM is connected to strong frontal systems driven by remote low pressure systems at higher latitudes over the North Atlantic. SREG is a combination of an inverted trough and a mid-tropospheric cold-core nearby Portugal. The statistical-dynamical modeling is based on logistic regressions (statistical component) developed for each regime separately (dynamical component). It is shown that the strength of the lightning activity (either strong or weak) for each regime is consistently modeled by a set of suitable dynamical predictors (65–70% of efficiency). The difference of the equivalent potential temperature in the 700–500 hPa layer is the best predictor for the three regimes, while the best 4-layer lifted index is still important for all regimes, but with much weaker significance. Six other predictors are more suitable for a specific regime. For the purpose of validating the modeling approach, a regional-scale climate model simulation is carried out under a very intense lightning episode.

© 2013 Elsevier B.V. All rights reserved.

1. Introduction

Cloud-to-ground discharges/flashes (hereafter CGD) are among the most noteworthy atmospheric hazards. CGD are dangerous events not only because they are potentially lethal and often cause human losses (Curran et al., 2000), but also due to the damages they may cause on the electric distribution networks and on the telecommunication systems (Mills et al.,

2010). Further, CGD can severely affect the aeronautic activity (Librantz and Librantz, 2006) or trigger forest fires by providing their ignition (García-Ortega et al., 2011; Rorig and Ferguson, 1999). Therefore, the study of the physical mechanisms underlying the CGD occurrence is of practical applicability in many fields, such as in electrical network planning. Many techniques are used for CGD detection, combining changes in the electromagnetic fields, in luminosity or electric current, among others. This detection can be provided either by sensors on board satellites (Christian et al., 1999) or by ground equipment like lightning sensors in weather stations (Cummins and Murphy, 2009).

The CGD are produced by thunderstorms and their statistical modeling has been carried out in a large number

* Corresponding author at: Instituto Português do Mar e da Atmosfera, Centro de Coordenação de Viseu, Estrada do Aeródromo, P.O. Box: 3515-342, Viseu, Portugal. Tel.: +351 232 450 852.

E-mail addresses: joao.sousa@ipma.pt (J.F. Sousa), mfragoso@campus.ul.pt (M. Fragoso), susana.mendes@gfi.uib.no (S. Mendes), jmcr@uevora.pt (J. Corte-Real), jsantos@utad.pt (J.A. Santos).

of studies (e.g. Burrows et al., 2005; Haklander and Van Delden, 2003), especially aiming forecast purposes. Sánchez et al. (2001) developed a short-term forecast model by using a logistic function as a binary forecasting technique determining storm/no storm occurrences in the province of León (Spain). More recent studies focusing on thunderstorm forecasting followed a similar methodology (e.g. Sánchez et al., 2008a, 2008b). In those binary forecast approaches a relationship is established between a predictand, i.e. the occurrence of a thunderstorm or hail fall, and a set of predictors, generally comprising a number of meteorological variables and stability indices. The number of lightning discharges has also been considered as a predictand in other logistic regressions (e.g. Mazany et al., 2002; Shafer and Fuelberg, 2006) or in other statistical models, such as tree-structured regressions (e.g. Burrows et al., 2005).

The lightning activity over Southern Europe has been analyzed in many previous studies (e.g. Altaratz et al., 2003; Defer et al., 2005; Shalev et al., 2011; Ziv et al., 2009). Despite the relative shortness of the lightning datasets in the Iberian Peninsula (IP), several studies have been carried out on its lighting activity. Rivas-Soriano et al. (2001a, 2005) characterized the spatial-temporal distribution of CGD over the IP. The correlation between convective precipitation and CGD over Iberia was also analyzed (Rivas-Soriano et al., 2001b). The lightning activity over IP was also related to the NAO (Rivas-Soriano et al., 2004; De Pablo and Rivas-Soriano, 2007). Other studies were more focused on regional to local features (e.g. Areitio et al., 2001, for the Basque country; Rivas-Soriano et al., 2001c, for inner Iberia). The effects of small urban areas and of the sea surface temperatures in the CGD distribution over Iberia were also analyzed by Rivas-Soriano and De Pablo (2002).

In Portugal, however, few studies have been devoted to this topic of research. The impacts of the CGD on power production infrastructures in Portugal were assessed by Rodrigues et al. (2009), while their impacts on the energy distribution networks were addressed by Almeida et al. (2009). The spatial and temporal distributions of the CGD over Portugal for the period 2003–2009, as well as their association with circulation weather types (Trigo and DaCamara, 2000), were first presented by Ramos et al. (2011). Santos et al. (2012) extended this analysis not only by improving the analysis of the CGD variability, but also by isolating three atmospheric regimes specifically related to the lightning activity in Portugal. Their results are in overall agreement with the preceding studies, including those for Spain. This study also highlighted the strong daily cycle, with the CGD occurrences peaking on mid-late afternoon, as well as the strong seasonality, with maximum activity in the summertime period, from May to September. Furthermore, it was shown that during the wintertime period, from October to April, two lightning regimes can be clearly identified, whereas in the summertime period (May–September) a single lightning regime is discernible. The winter remote regime (WREM) is typically characterized by frontal systems crossing Portugal and associated with remote low pressure systems northwards of the IP. Conversely, cut-off lows located over or nearby the IP characterize the winter regional regime (WREG). Lastly, the summer regional regime (SREG) features inverted shallow troughs, extending from North Africa towards Portugal, which are concomitantly accompanied by mid-tropospheric cold cores over the region.

The objectives of the present study are threefold: (1) deepening the characterization of the dynamical structure of the three lightning regimes found by Santos et al. (2012), considering other atmospheric fields and higher-resolution datasets; (2) implementing an innovative statistical-dynamical modeling of the CGD by using the knowledge about the physical nature of the different lightning regimes in Portugal; (3) validating the modeling approach using a high-resolution regional-scale climate model simulation for an extreme lightning episode. Section 2 will be devoted to the description of the datasets and methodologies. In Section 3 the results are presented and discussed. Finally, an overview of the main results is presented in Section 4.

2. Material and methods

CGD data over Portugal are collected by the Portuguese lightning detection network (hereafter LDN), which is maintained by the national weather service (Instituto Português do Mar e da Atmosfera; IPMA) and it was installed in June 2002. The Portuguese LDN comprises four IMPACT 141 T-ESP sensors (Carvalho et al., 2003; Ramos et al., 2007) assembled in order to cover the whole of mainland Portugal (cf. Santos et al., 2012, their Fig. 2). The Spanish LDN, with 14 sensors, is maintained by the Spanish Meteorological Agency (AEMET) and complements the Portuguese LDN through data interchange. This strategic cooperation allows a joint efficiency of first-stroke detection on the Iberian LDNs of about 90% for CGD with discharge peak currents higher than 5 kA and over the entire IP (Rodrigues et al., 2010). Data is currently available over the period 2003–2009 (7 years). The raw data is gridded onto a regular 0.10° latitude \times 0.10° longitude grid, corresponding to a spatial resolution of nearly 10 km. The gridded CGD density (in CGD km^{-2}) is then computed using the respective grid box area. Further details about this network and its corresponding sensors can be found in Santos et al. (2012).

Both the dynamical characterization of the lightning regimes in Portugal and the statistical modeling employ gridded atmospheric fields. The state-of-the-art high-resolution *Modern Era Retrospective-analysis for Research and Applications* (MERRA) reanalysis dataset is used for this purpose (Rienecker et al., 2011). This dataset was produced by the *Modelling and Assimilation Data and Information Services Center* (MDISC), which is maintained by the *NASA Goddard Earth Sciences* (GES) *Data and Information Services Center* (DISC), and is available at their website (<http://disc.sci.gsfc.nasa.gov/>). The mean sea level pressure (MSLP) and the geopotential height (HGT), zonal (U) and meridional (V) wind components, temperature (T), relative humidity (RH), specific humidity (q) and potential vorticity (PV) at 850, 700, 500 and 300 hPa are retrieved from the MERRA database, a 6-hourly dataset on a 0.50° latitude \times 0.67° longitude grid.

In order to improve the aforementioned dynamical characterization, other atmospheric parameters not available in the MERRA dataset are also used herein. The 10 m U and V are obtained from the Japanese reanalysis dataset (JRA; Onogi et al., 2007), produced by the *Japan Meteorological Agency* (JMA)–*Central Research Institute of Electric Power Industry* (CRIEPI). These parameters are available over a 1.25° latitude \times 1.25° longitude grid at a 6-hourly time scale. Further, the best 4-layer lifted index (LI) from the *National Centers for Environmental*

Prediction Final Operational Model Global Tropospheric Analyses (NCEP FNL) is supplied by the *University Corporation for Atmospheric Research* (UCAR) and is available at a spatial resolution of 1.0° latitude $\times 1.0^\circ$ longitude and at 6-hour intervals (<http://rda.ucar.edu/datasets/ds083.2/>). This operational data is generated by the *Global Data Assimilation System* (GDAS), which continuously collects observational data from different sources. The *LI* is a measure of the difference between the environment and parcel temperatures at 500 hPa and represents the net buoyancy force (negative upwards).

The Weather Research and Forecasting, WRF model (Skamarock and Klemp, 2007; Skamarock et al., 2008) is used for simulating high-resolution atmospheric fields during a strong lightning activity episode in Portugal, which occurred between 10 and 17 of September 2007. Some studies were performed in the Mediterranean, using the WRF in order to predict the lightning distribution (Lynn and Yair, 2010; Yair et al., 2010). The influence of the initial conditions on lightning forecasting using the WRF was also verified by Zepka et al. (2012). The WRF is commonly used in meso and micro-scale studies (Soares et al., 2012), mainly because it allows working with fine grid resolutions, obtaining therefore a better simulation of orographic effects, which are very important in the spatial distribution of CGD. In the present study, the WRF is set up with 3 horizontal domains (Fig. 1). For the parent domain (1) the simulations have a horizontal grid spacing of 60 km, while for the other two nested domains they have (2) 20 km and (3) 4 km of grid spacing. The vertical domain is composed of 29 levels with the model top at 30 hPa. A summary of the datasets used in the present study is listed in Table 1.

As in Santos et al. (2012), a CGD day presents at least 25 CGD recorded over Portugal, which is the median of the non-zero daily discharges in 2003–2009. This threshold is used so that only days with important lightning activity over Portugal are retained for the identification of the lighting

regimes. In fact, less than 25 CGD over the total area of Portugal is considered a day with low activity. Although some of these CGD can present relatively high peak currents, they are commonly localized over very narrow areas of the country, thus not being representative of the whole country and difficult to relate to large-scale atmospheric regimes. A K-means clustering analysis (Wilks, 2006) is applied to the first five principal components (PC) of the daily mean fields of the MSLP within the Euro-Atlantic sector (25° – 65° N; 30° W– 10° E) and only for the CGD days (376). These PC cumulatively represent about 92% of the total temporal variance of the MSLP fields for CGD days. The analysis is also applied to the winter (October–April; 7 months) and summer (May–September; 5 months) periods separately. As is described in detail by Santos et al. (2012), these periods are chosen according to the seasonal cycle of the CGD in Portugal. Three lightning regimes are identified: WREG, WREM and SREG. Despite of using the MERRA MSLP, instead of the JRA 1000 hPa geopotential height (as in Santos et al., 2012), the same regimes are eventually identified here for the same set of CGD days (a total of 376 days, 190 in winter and 186 in summer). A total of 122 days are classified as WREG and 68 to the WREM (instead of 115 and 75 as in Santos et al., 2012). In summer, all 186 CGD days are classified as SREG.

Multivariate regression modeling is then applied to each regime separately in order to take into account their different dynamical structures, leading thus to an innovative statistical-dynamical modeling approach. Several candidate predictors are tested in these models, using all the aforementioned variables, as well as other derived variables, such as the moist static stability index, SSI, defined as:

$$\text{SSI} = -1/\theta_e(\partial\theta_e/\partial p)$$

where θ_e is the equivalent potential temperature and p the pressure level. θ_e is estimated using the approximate expression $\theta_e \approx (T + L_v q/c_p)(1000/p)^k$, where T is the air

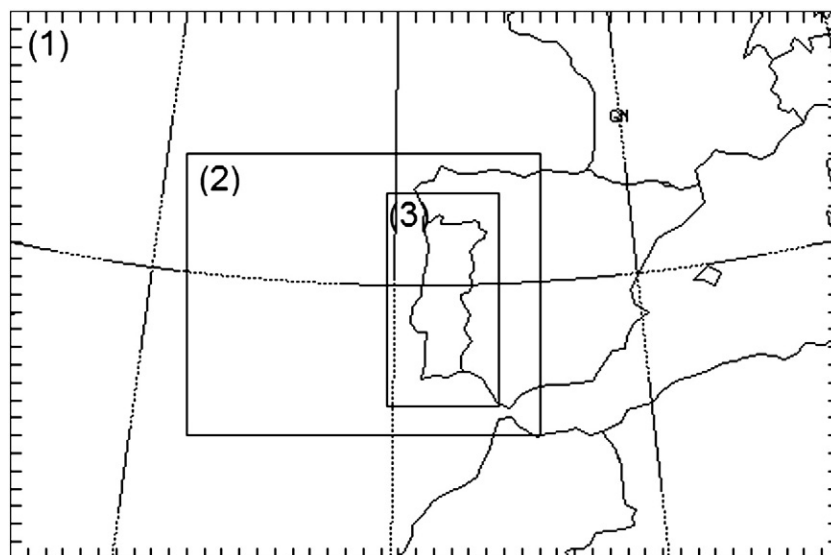


Fig. 1. Map showing the parent (1) and the two nested (2) and (3) horizontal domains used in the WRF simulation for the episode 10–17 September 2007. Domain (1) has 60 km, (2) 20 km and (3) 4 km of grid spacing.

Table 1

Summary of the datasets used in the present study, along with the selected variables (and acronyms), levels, grid resolution, time resolution, and their methodological applications.

| Dataset | Variables | Acronyms | Levels | Grid resolution (lat × long) | Time resolution (hours) | Applications |
|----------------|----------------------------|----------|--------------------|---------------------------------|----------------------------|-----------------------------------|
| Portuguese LDN | Cloud-to-ground discharges | CGD | Surface | 0.10° × 0.10° | 1 | Regime characterization/modeling |
| MERRA-300 | Mean sea level pressure | MSLP | Surface | 0.50° × 0.67° | 6 | Regime characterization/modeling |
| DAS | Geopotential height | HGT | 850, 700, 500, 300 | | | |
| | Meridional and zonal wind | U, V | | | | |
| | Air temperature | T | | | | |
| | Relative humidity | RH | | | | |
| | Specific humidity | q | | | | |
| | Potential vorticity | PV | | | | |
| UCAR/GDAS | Lifted index | LI | | 1.00° × 1.00° | | Regime characterization/Modelling |
| JRA | Meridional and zonal wind | U, V | 10 m | 1.25° × 1.25° | 6 | Regime characterization |
| WRF simulation | Geopotential height | HGT | 700, 500 | 0.18° × 0.18° | 1 | Case study |
| | Air temperature | T | | | | |
| | Meridional and zonal wind | U, V | 10 m | 0.18° × 0.18° | 1 | |

temperature, q the specific humidity, $L_v = 2.465824 \times 10^6 \text{ J kg}^{-1}$ the vaporization latent heat, $c_p = 1004 \text{ J K}^{-1} \text{ kg}^{-1}$ the specific heat capacity at constant pressure and $k = 0.286$ the Poisson's constant. As such, a stable atmospheric layer has a $SSI > 0$. This index is calculated for the 850, 700, 500 and 300 hPa levels and the partial derivatives are estimated by centered finite differences.

The WRF parameterizations are now shortly described. The single-moment 6-class microphysics scheme (WSM6) is set up on the 1st nested domain, and the Morrison double-moment scheme on the 2nd nested domain. The WSM6 microphysics scheme includes graupel and related processes, as well as mixed-phase particle fall speeds for the snow and graupel particles, through a new method developed by Hong and Lim (2006). The Morrison et al. (2009) microphysics scheme is a double-moment scheme that includes six species of water: vapor, cloud droplets, cloud ice, rain, snow and graupel/hail. The number concentrations and the mixing ratios of several hydrometeors are the prognostic variables. The prediction of the number concentration and mixing ratio fields improves the particle size distributions, which are fundamental for calculating the microphysical process rates and evaluate the precipitation processes. The $20 \text{ km} \times 20 \text{ km}$ nested horizontal domain uses the Grell-3D cumulus scheme (Grell and Devenyi, 2002), which allows subsidence effects to be spread to neighboring grid columns, being also effective on larger grid sizes, where subsidence occurs within the same grid column as the updraft. The cumulus parameterization was turned off for the $4 \text{ km} \times 4 \text{ km}$ domain, because the model can resolve the drafts by itself in this domain. For the present case study, the three horizontal domains are set to the Noah Land-Surface model (Chen and Dudhia, 2001). The parent domain uses the Mellor-Yamada-Janjic (Janjic, 2002) planetary boundary layer (PBL) scheme, which parameterizes the turbulence in the PBL and in the free atmosphere. The Yonsei University PBL scheme (Hong et al., 2006) is activated for both nested horizontal domains. It represents the fluxes due to non-local gradients and explicitly considers the entrainment layer at the top of the PBL. The initial and lateral boundary conditions are given by the NCEP FNL Operational Model Global Tropospheric Analyses. The available simulations employ the Shuttle Radar Topography Mission (SRTM) digital elevation data, a high-resolution

topography dataset with 90 m of horizontal resolution; available at <http://srtm.csi.cgiar.org/SELECTION/inputCoord.asp>.

3. Results

3.1. Lightning regimes

As previously described, this study analyses three distinct lightning regimes in Portugal, namely WREG, WREM and SREG. The WREG is characterized by a low pressure system westwards of the IP and a blocking high pressure over the British Isles (Fig. 2a). This regime is associated with strong cyclonic activity inducing southerly and westerly winds over Portugal. These dynamical conditions can trigger important lightning activity in Portugal, particularly over its southern half (cf. composite of the CGD density in Fig. 2a). The WREM presents a strong trough over Portugal, suggesting intense frontogenesis, accompanied by southwesterly flow over the country (Fig. 2b). The corresponding CGD density shows a relatively spread pattern, with occurrences throughout the country, but again more concentrated over southern Portugal (Fig. 2b). The SREG is related to an inverted low pressure trough over Portugal, with a significant wind convergence near northern Portugal (Fig. 2c), which generates air parcel rising. The respective CGD pattern depicts high CGD densities over inland areas, while relatively low densities can be found along the coastal areas (Fig. 2c).

The mid-tropospheric cold-core in the WREG is evident in both the 500 hPa geopotential height and temperature, displaying a nearly barotropic equivalent structure, i.e., geopotential lines almost parallel to the isotherms above the surface low pressure system (Fig. 3a). A clear core of cyclonic vorticity in the low pressure area and the wide anticyclonic area at higher latitudes are also noteworthy (Fig. 3a). This vorticity pattern sustains the intense cyclogenesis that usually prevails during WREG. The 500 hPa fields for the WREM hint at a strong trough westwards of Portugal (westward vertical tilting), which is accompanied by intense baroclinicity and a large area of positive vorticity, extending from the high latitudes of the North Atlantic towards Portugal (Fig. 3b). The SREG displays a mid-tropospheric cold-core over Portugal, which greatly contrasts

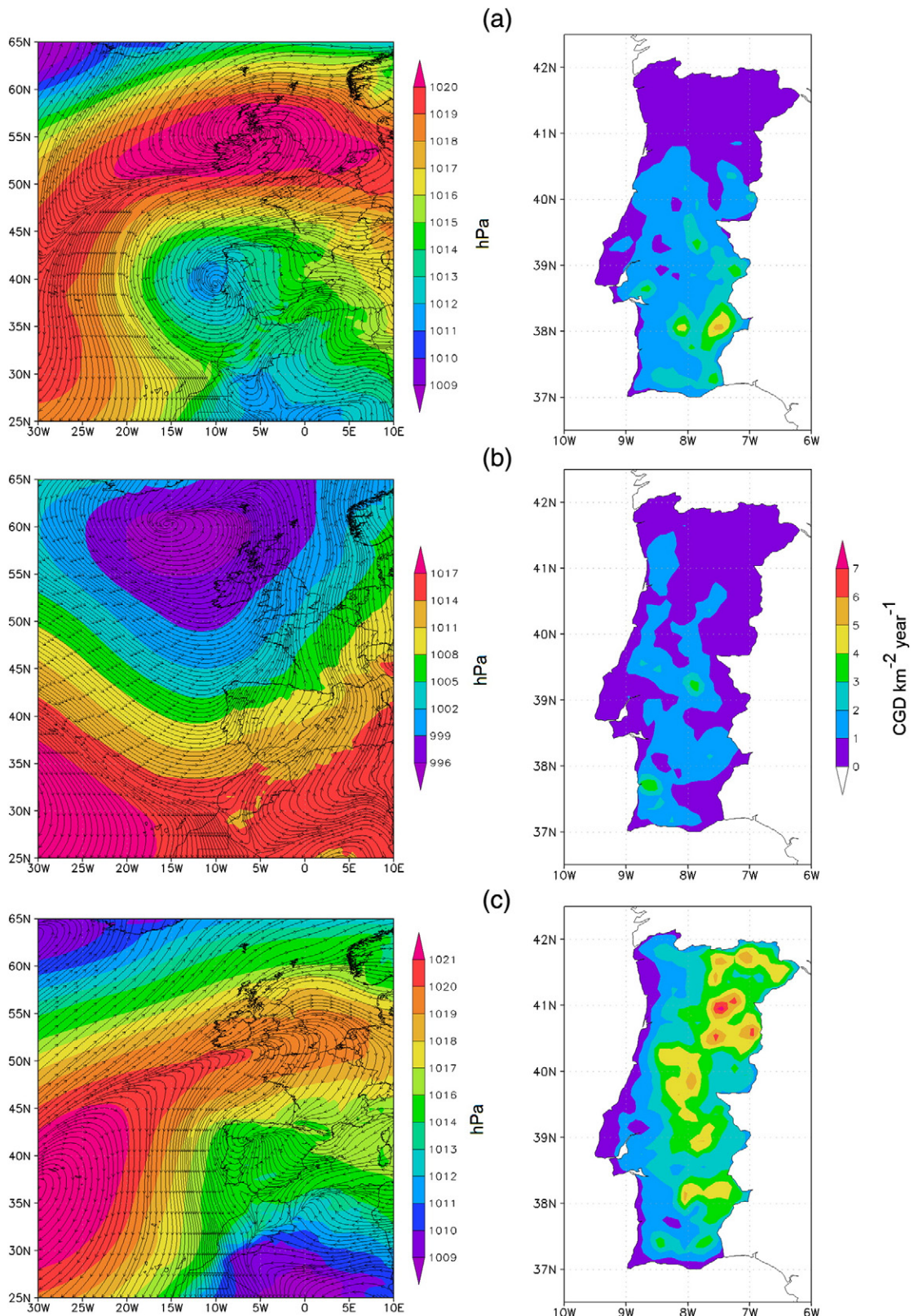


Fig. 2. Left panels: Composite patterns of the daily mean MSLP (shading in hPa) and streamlines of the 10 m horizontal wind (m s^{-1}) of the three CGD regimes over mainland Portugal in 2003–2009: (a) WREG; (b) WREM; (c) SREG. Right panels: Corresponding mean patterns of the CGD density ($\text{CGD km}^{-2} \text{ year}^{-1}$) after applying a 0.5° latitude \times 0.5° longitude kernel smoothing.

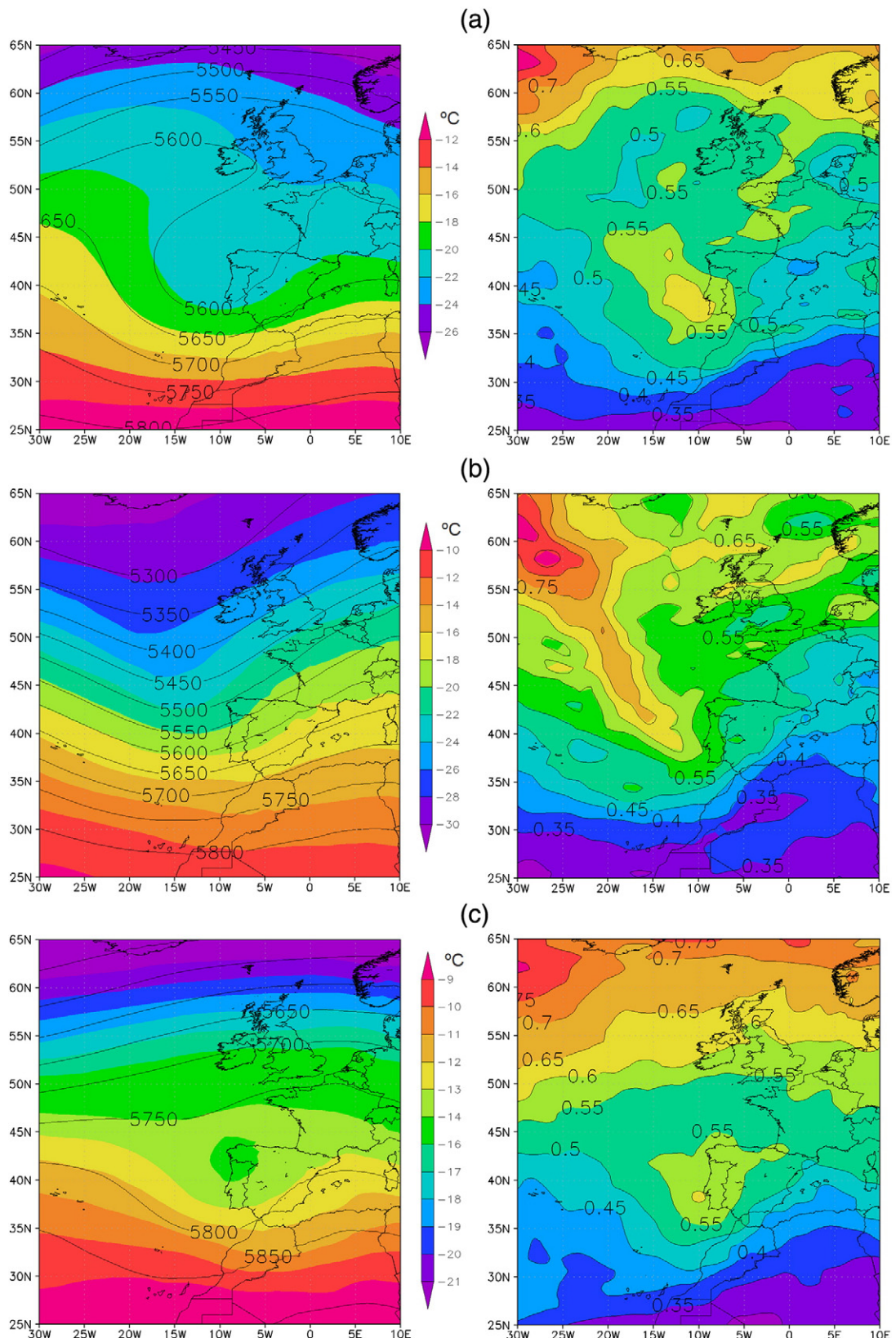


Fig. 3. As in Fig. 2, but now for the composites of the air temperature (shading in °C) and geopotential height (contours in gpm) at 500 hPa (left panels) and potential vorticity (PVU) at 500 hPa (right panels) for the: (a) WREG; (b) WREM; (c) SREG.

with the near-surface high temperatures, triggering strong vertical instability and explaining the intense lightning activity (Fig. 3c). The corresponding 500 hPa vorticity field reveals a pattern similar to that of the WREG (Fig. 3a, c), though weaker, narrower and located south-westwards of Portugal. In fact, the vorticity field at different pressure levels clearly substantiates the denominations of the regimes as regional or remote.

3.2. Statistical modeling

In order to relate the strength of the lightning activity in Portugal to atmospheric parameters, daily totals of the CGD summed over Portugal and for each regime (only CGD days are considered) are used for this purpose. Local (point-by-point) CGD occurrences are not considered herein, but rather their sum over the whole of the country. In fact, a preliminary exploratory analysis of the local CGD series using multivariate statistical tools, such as canonical correlation analysis, has not revealed robust coupling patterns between these local

series and large-scale atmospheric fields. This can be largely explained by the small sample size of the dataset (7 years). Therefore, a point-by-point modeling is out of the scope of the present study.

Nevertheless, their very high positive skewness is a major shortcoming for statistical modeling (Fig. 4), as the application of many stochastic methods relies on symmetry-related assumptions. As such, Box–Cox transformations are tested so as to identify the best transformations to symmetrize the distributions (Wilks, 2006). According to this methodology, the natural log-transformation is chosen. As expected, the transformed variables are much more symmetric than the raw variables (Fig. 4). The log-transformed CGD (hereafter LCGD) daily totals for each regime are then considered as predictands of the strength of the lightning activity in Portugal.

The previous analysis of the prevailing dynamical structure of each of the three lightning regimes demonstrates that they are not mere statistical artifacts, but they do represent well-defined regimes of the atmospheric flow, exhibiting

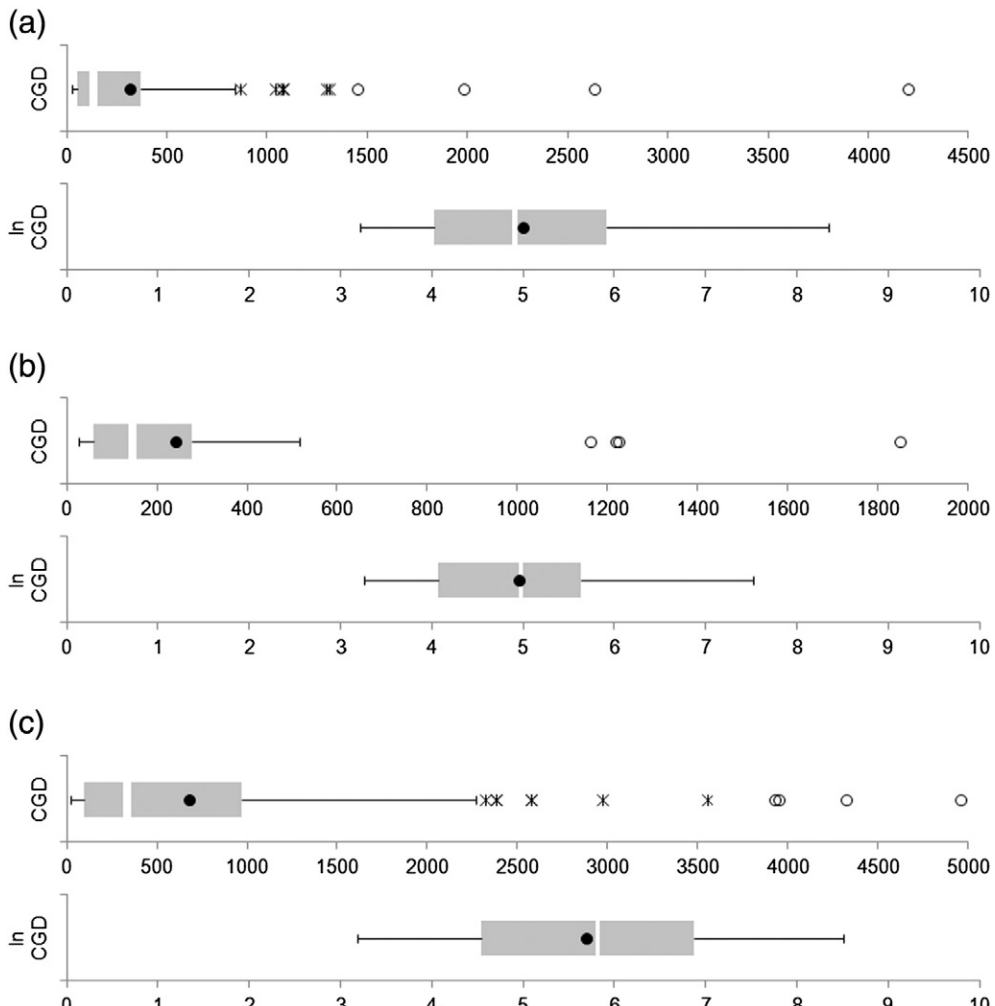


Fig. 4. Box-plots of the CGD daily occurrences (upper panels) and of their natural logarithms (lower panels) for the: (a) WREG; (b) WREM; (c) SREG. Left (right) box limits correspond to the 25th (75th) percentiles, white vertical lines to medians, black circles to means and whisker limits to non-outlier minima and maxima. Asterisks (circles) are 1st (2nd) order outliers.

Table 2

Selected predictors by the stepwise approach for each multivariable linear regression model of each regime (WREG, WREM and SREG, see text for details). The rank of the selection is also indicated by numbers. The correlation coefficient between the observed and modeled daily LCGD series over Portugal, r , as well as the corresponding determination coefficient (percentage of variance in the observed daily LCGD series represented by the model) after applying a 1-step cross-validation, r_{cv}^2 , and the p -level of the Fisher hypothesis testing (from ANOVA) are also listed for each regime/model.

| Regime | Predictors | | | | | | | | Model statistics | | |
|--------|----------------------------|-------|-----------------------|-------------|------------------|------------|------------|----------------------|------------------|----------------|------------|
| | $\Delta\theta_{eq700-500}$ | LI | $\Delta RH_{700-500}$ | SSI_{700} | θ_{eq300} | PV_{700} | PV_{500} | $\Delta q_{700-500}$ | r | r_{cv}^2 (%) | p -level |
| WREG | 1 (+) | 3 (-) | | | | | | 2 (+) | 0.46 | 19 | <0.001 |
| WREM | 1 (+) | 4 (-) | 2 (-) | 3 (-) | | | | | 0.60 | 32 | <0.001 |
| SREG | 1 (+) | 4 (-) | | | 2 (-) | 5 (+) | | 3 (+) | 0.58 | 32 | <0.001 |

physically meaningful patterns. Therefore, aiming at improving the current understanding of the lightning activity in Portugal, a country with Mediterranean-type climates under strong Atlantic influences, a large number of atmospheric variables are tested as potential predictors of the LCGD.

As simple statistical approaches, multivariate linear regressions, with stepwise variable selection, are first applied to the LCGD totals to isolate the most relevant predictors. By considering the stepwise selection, eight predictors are chosen (Table 2). Although the stepwise methodology already takes into account the collinearity between regressors, the Belsley Collinearity Diagnostics (cf. Belsley et al. 1980) confirms the low collinearity levels in the three models/regimes (Table 3). The area-means, within the Portuguese sector (6–10°W; 37–42°N; PS henceforth), of the 700–500 hPa differences in the equivalent potential temperature ($\Delta\theta_{eq700-500}$), specific humidity ($\Delta q_{700-500}$), relative humidity ($\Delta RH_{700-500}$), and of the 300 hPa equivalent potential temperature (θ_{eq300}) are considered. In addition, the maximum potential vorticity at 700 hPa (PV_{700}) and 500 hPa (PV_{500}), the minimum SSI at 700 hPa (SSI_{700}) and the minimum LI within the PS are also selected. Other variables were also tested, but their modeling skills are low and are not selected by the stepwise method in any of the three regimes, then being discarded in this study. The modeling statistics are presented in Table 2.

The WREG model uses three predictors ($\Delta\theta_{eq700-500}$, LI and PV_{500}) and has a correlation coefficient between the observed and modeled daily LCGD series over Portugal of 0.46, representing 19% of the total variance of the observed daily LCGD series, after applying a 1-step cross-validation (Table 2). Hence, despite having a statistically significant model, the percentage of explained variance is low, which highlights the rather complex nature of the lightning activity during this regime. For the WREM, however, four predictors

are selected ($\Delta\theta_{eq700-500}$, LI , $\Delta RH_{700-500}$ and SSI_{700}) and the correlation coefficient is of 0.60; the percentage of represented variance after cross-validation is of 32% (Table 2). Finally, for the SREG, five predictors are selected ($\Delta\theta_{eq700-500}$, LI , θ_{eq300} , PV_{700} and $\Delta q_{700-500}$) and the correlation coefficient is now of 0.58, the model explaining about 32% of the total variance after cross-validation. Despite these modest skills, the three models are statistically significant according to the Fisher's test (statistical significance below 0.1%; Table 2).

The order of relevance of each predictor, according to the stepwise method, is also listed along with the sign of the corresponding regression coefficient (Table 2). These results allow concluding that the leading predictor is $\Delta\theta_{eq700-500}$ in the three regimes, which means that anomalously high differences between 700 and 500 hPa equivalent potential temperatures (positive sign of the regression coefficient) are globally favorable to high LCGD totals. Therefore, weak or inverted vertical gradients of the equivalent potential temperature trigger convective instability, which in turn tends to induce lightning activity. In fact, the 700–500 hPa layer plays a key role on the development of thunderstorm convective cells. The LI is also a significant predictor for the three regimes (Table 2). Anomalously low LI values (mid-tropospheric upward buoyancy force) tend to favor high LCGD totals, though its relevance is interestingly not as great as it would be expected. The relevance of these two predictors is particularly clear in the WREG (Figs. 2a and 3a).

In the WREM, the LCGD totals are also favored by anomalously low differences in the relative humidity for the 700–500 hPa layer and by anomalously low SSI_{700} (Table 2). Thereby, high humidity values throughout the low and mid troposphere are clearly favorable to high LCGD totals in this frontal regime. This result is indeed in accordance with the presence of a well-developed frontal line over Portugal, with abundant moisture and saturated air masses extending from the surface to the upper troposphere. Low static stability at the low troposphere (SSI_{700}) also plays a key role on triggering high LCGD totals in this regime, which is once more in agreement with the presence of frontal lines, such as cold fronts. Overall, the selected predictors are supported by the dynamical features of the WREM (Figs. 2b and 3b). Lastly, during the SREG, anomalously low θ_{eq300} and anomalously high PV_{700} and $\Delta q_{700-500}$ are also important predictors of the LCGD totals. The lightning activity is thus mostly potentiated by anomalously high humidity and potential vorticity at the lower troposphere, fundamental conditions to provide the required moisture for the development of deep convection and lightning. Moreover, the presence of cold air masses at upper tropospheric levels (θ_{eq300}) can also play a key role in triggering the deep convection. These

Table 3

Condition indices for each regime and for the selected regressors as they are cumulatively incorporated in each model. According to the Belsley Collinearity Diagnostics (cf. Belsley et al. 1980), these indices must be preferably below 30 (commonly used as the default tolerance) in order to neglect collinearity in the models.

| WREG | WREM | SREG |
|----------------------------|------|----------------------------|
| LI | 1.0 | SSI_{700} |
| $\Delta\theta_{eq700-500}$ | 2.8 | LI |
| PV_{500} | 4.3 | $\Delta RH_{700-500}$ |
| | | $\Delta\theta_{eq700-500}$ |
| | | PV_{700} |
| | | 10.3 |
| | | 19.6 |

outcomes are again in close conformity with the dynamical features of this regime (Figs. 2c and 3c).

The previous outcomes highlight the extreme complexity encompassed by the LCGD modeling. Despite the moderate skills obtained by the linear regression models presented above, they provide a set of valuable predictors that can ultimately be used in other statistical modeling approaches. In fact, one main reason for the weakness of the previous relationships is due to the high irregularity and unpredictability of the CGD totals, as they are also strongly controlled by meso and micro-scale mechanisms, induced e.g. by thermal contrasts, orography and land use/cover. Furthermore, from an operational viewpoint, instead of predicting the exact number of CGD over Portugal, it is more relevant to predict if the lightning activity will be strong or weak. As such, a logistic regression model, using the same predictors selected for the linear regressions, is developed for each regime so as to model the probabilities of occurrence of two classes: CGD < P50 (low activity) and CGD ≥ P50 (high activity), where P50 is the median of each distribution (Table 4). It is worth noting that the classification of each day into these two classes remains unchanged either using LCGD or CGD (the logarithmic scaling will not change the ranking of the days in the time series).

In the logistic modeling, for each day of each regime two probabilities are obtained, one for each of the two classes referred above (low/high activity); the sum of these two probabilities is equal to 100% by definition. Days are then keyed to the highest probability class. The efficiencies of each model are calculated as the percentages of correct correspondences between the modeled and the observed classes for all days of each regime (Table 4). The total efficiencies are of 70% (WREG), 65% (WREM) and 67% (SREG), which are reasonably high skills that can be used as a complement in operational weather forecasting.

3.3. Dynamical diagnosis

The dynamical feasibility of the previously selected predictors is now discussed by analyzing their composites for each regime and their composites of the differences between each regime and the days without CGD. With respect to the composites of $\Delta\theta_{eq700 - 500}$ it can be confirmed that anomalously high values are registered over Portugal, mainly in the SREG, with a core anomaly above 5.5 °C in northeastern Portugal (Fig. 5c). This pattern partially explains the greater lightning activity in the summer period (May–September),

particularly over northern Portugal, where both the CGD and the $\Delta\theta_{eq700 - 500}$ show maxima (Figs. 2c and 5c). In fact, the median (P50) of the CGD is more than two times higher in the SREG (346 CGD day⁻¹) than in the WREG/WREM (135/145 CGD day⁻¹; Table 4). Regarding the composites of θ_{eq300} , they depict anomalously low values in both WREG and SREG (Fig. 6a,c), which is in agreement with the associated cold-core low pressure systems extending throughout the troposphere (Figs. 2 and 3). This feature is particularly clear for the SREG, justifying the inclusion of this predictor in the CGD statistical modeling for this regime (Table 2). In the WREM, nevertheless, no significant anomalies are detected (Fig. 5b), as most of the frontal systems do not present clear signatures at the upper tropospheric levels.

The composites for the humidity parameters $\Delta RH_{700 - 500}$ and $\Delta q_{700 - 500}$ show no clear dependence on the WREG (Fig. 6a). In fact, none of the two are predictors for this regime (Table 2). Nonetheless, distinct positive anomalies can be found in both WREM and SREG (Fig. 6b, c), particularly in the SREG, being $\Delta RH_{700 - 500}$ more relevant for the WREM and $\Delta q_{700 - 500}$ for the SREG (Table 2). Furthermore, it is still worth mentioning that the location of the maximum in $\Delta q_{700 - 500}$ is over north and central-inner Portugal for the SREG, the region with higher CGD occurrences and higher $\Delta\theta_{eq700 - 500}$ anomalies (Figs. 2c and 5c). There is also some redundancy between the two humidity parameters, explaining the fact that they are not jointly selected by the stepwise method for the same regime (Table 2). The composites for the LI display negative anomalies across Portugal (Fig. 7), attesting the relatively high skill of this predictor in modeling the CGD occurrences in the three regimes (Table 2). Although the composites for the SSI₇₀₀ also display negative anomalies over the country and for the three regimes (Fig. 7), this predictor is selected by the stepwise method only for the WREM (Table 2).

3.4. Case study

In this section, a case study is analyzed for the purpose of validating the previously presented statistical-dynamical modeling approach. The episode with strongest electrical activity over Portugal in the period of 2003–2009 is chosen for this goal (10–17 of September 2007). All episode days are keyed as SREG days. In both the day before the onset of this episode (9 of September) and the day after its decay (18 of September), the daily CGD recorded over Portugal were below the median (346 CGD day⁻¹) of the full distribution for SREG (Fig. 8). CGD occurrences below this median are in effect the chosen criterion for defining the onset and decay of the episode. Concerning the daily distribution of the lightning activity during the episode, the CGD totals over Portugal show a maximum occurrence on the 10th of September (4952 CGD; the absolute maximum of CGD totals in Portugal), a sharp decrease in the following two days and some stationarity at values around 1500 CGD day⁻¹ until the end of the episode (17 of September). For the whole episode the number of CGD largely exceeds the median of the full distribution for SREG (346 CGD day⁻¹). As such, at the end of this episode, a total of 16,873 CGD were recorded, confirming its strong lightning activity.

The probabilities of the class CGD ≥ P50 across the case study are also displayed in Fig. 8. The probabilities of the class

Table 4

Efficiencies of the logistic models (percentages of correct correspondences between the modeled and the observed classes over all days of each regime). Two non-overlapping classes are considered in these models: CGD < P50 and CGD ≥ P50, where P50 is the median of the time series of the daily CGD totals, summed over Portugal, and for each regime separately. Their values are also listed.

| Regime | Efficiency (%) | P50 (CGD day ⁻¹) |
|--------|----------------|---------------------------------|
| WREG | 70 | 135 |
| WREM | 65 | 145 |
| SREG | 67 | 346 |

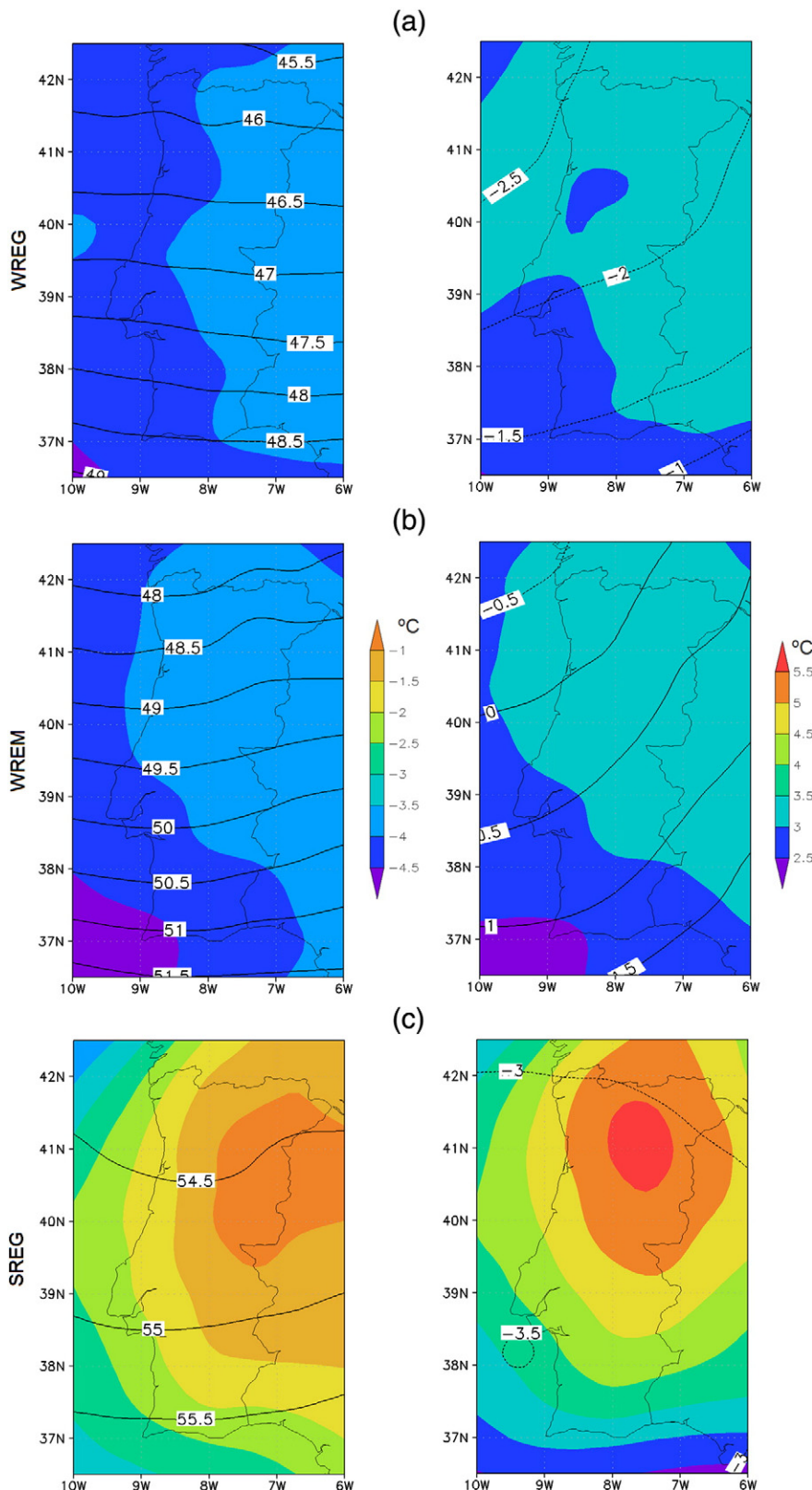


Fig. 5. Composite patterns of the daily mean difference of the equivalent potential temperature between 700 and 500 hPa ($\Delta\theta_{eq700 - 500}$; shading in °C) and daily mean equivalent potential temperature at 300 hPa (θ_{eq300} ; contours in °C): Left panel—(a) WREG, (b) WREM and (c) SREG; Right panel—Difference between left panel and days without CGD.

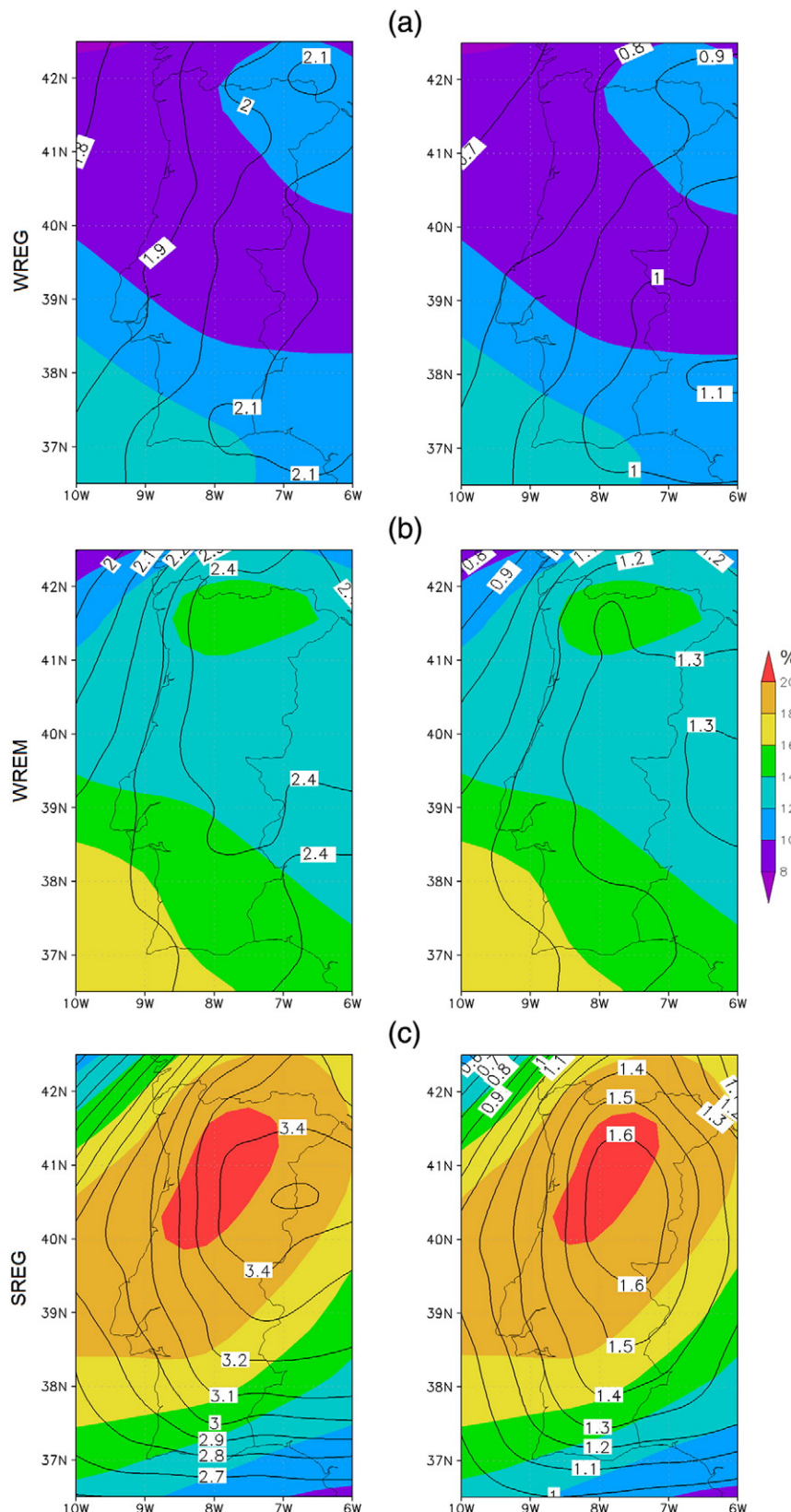


Fig. 6. Composite patterns of the daily mean difference of the relative humidity between 700 and 500 hPa ($\Delta RH_{700-500}$; shading in %) and same to the specific humidity ($\Delta q_{700-500}$; contours in g kg^{-1}): Left panel—(a) WREG, (b) WREM and (c) SREG; Right panel—Difference between left panel and days without CGD.

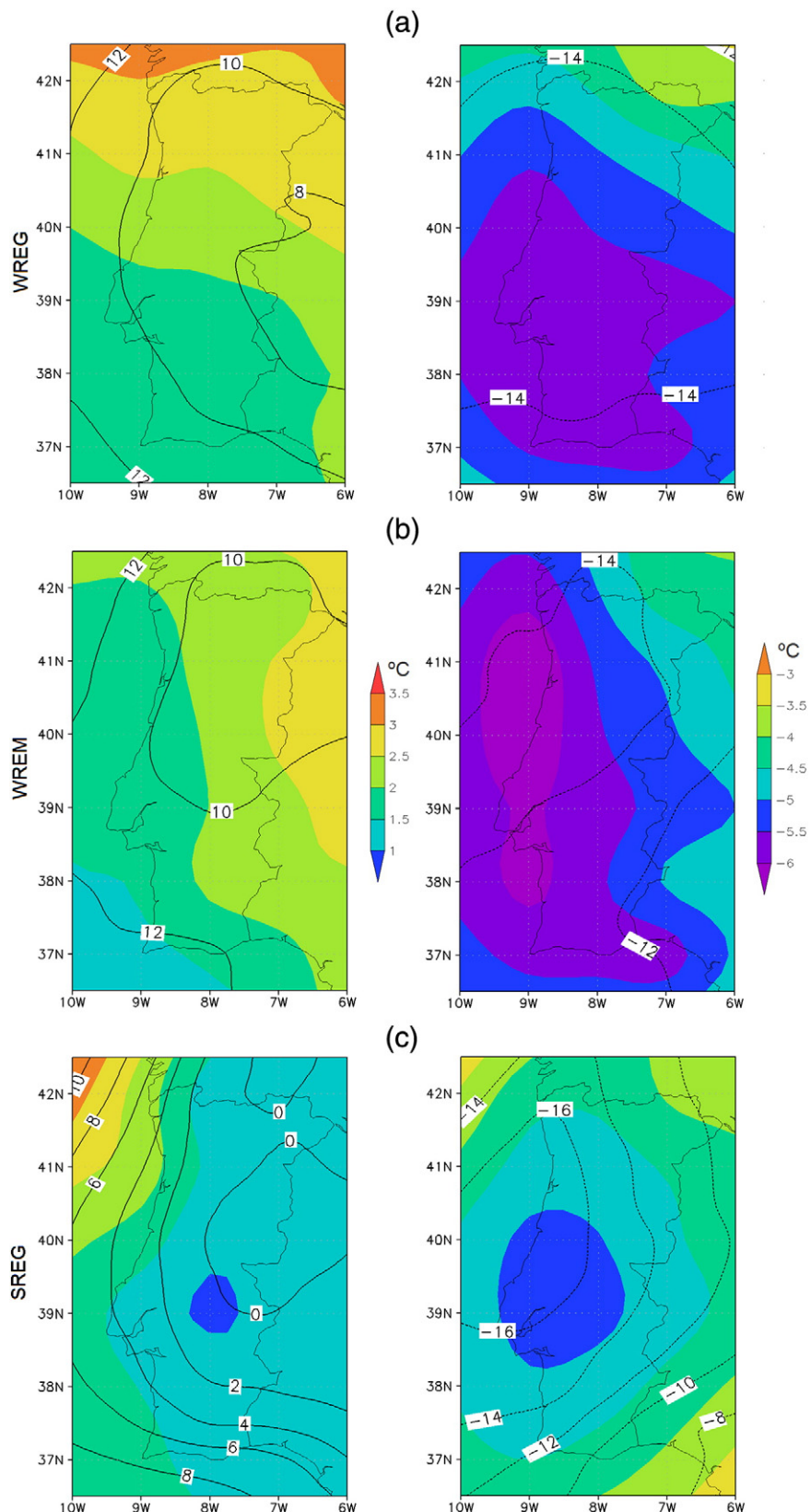


Fig. 7. Composite patterns of the daily mean best 4-layer lifted index (LI ; shading in $^{\circ}\text{C}$) and daily mean moist static stability index at 700 hPa (SSI_{700} ; contours in 10^5 hPa^{-1}): Left panel—(a) WREG, (b) WREM and (c) SREG; Right panel—Difference between left panel and days without CGD.

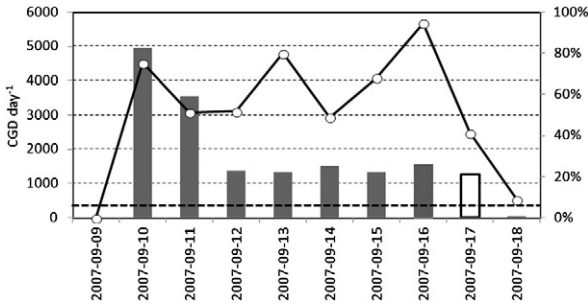


Fig. 8. CGD day⁻¹ (bars) and correspondent logistic model probability of the class CGD \geq P50 (black line with white circles) across the case study episode (10–17 September 2007). The day before its onset and the day after its decay are also shown. Dashed line indicates the CGD median in SREG (346 CGD day⁻¹; Table 4). The white bar (2007-09-17) represents an incorrect evaluation by the logistic model (i.e. probability of the class CGD \geq P50 below 50% when the CGD total is above the median).

CGD $<$ P50 are not shown as the sum of the two is equal to 100% by definition. The statistical–dynamical model correctly reproduces the class CGD \geq P50 (strong lightning activity) for all days, except on 17 of September (white bar in Fig. 8), when the model shows a higher probability for CGD $<$ P50 (i.e. probability of the class CGD \geq P50 below 50%), which was actually only verified in the following day. Nevertheless, it can be stated that the model is able to reliably reproduce the classes of lightning activity throughout this particular episode, as well as its onset (high probability for CGD \geq P50 in the onset day) and its decay (steep decrease in the CGD $<$ P50 probability from 16 to 18 of September). Furthermore, these outcomes also hint at the ability of the few selected dynamical predictors/precursors in predicting the observed lightning activity, despite the complexity inherent to its underlying physical mechanisms.

The spatial distribution of the daily CGD totals over Portugal (Fig. 9) clearly shows an explosive activity at the beginning of the episode over the southern half of Portugal (10 of September), characterized by two maxima cores, one over the southwesternmost corner (mountain ranges near Monchique) and another much farther to the north, in the region of Alto Alentejo. In the second day (11 of September), a northward displacement of the lightning activity is clear, with its reinforcement over Alto Alentejo. In the two following days (12–13 of September), this northward drift is more pronounced, with strong activity found over northeastern Portugal, though important activity still remains over southern Portugal. The lightning activity remains intense in the following days, but widely scattered over most of the country, with its daily maxima undergoing several migrations. Overall, significant lightning activity was recorded across Portugal (Fig. 9), which means that this episode was not only strong, but also spread over the country.

An analysis of the synoptic charts for this episode provides some important clues (Fig. 10). In the period of 10–12 of September, a strong high pressure system (1033–1031 hPa) centered over the Eastern Atlantic, at 50°N latitude, is noteworthy. The influence of this anticyclone reached to the British Islands and France by the 12 of September. In addition, a weak (1017–1019 hPa) low pressure over the southern IP, connected with the thermal low centered over North Africa is also noticeable. The lower troposphere over the Portuguese

area is affected by easterly or southeasterly winds, bringing in warm air from the inner regions of Spain or from Northern Africa, respectively. For the period of 13–14 of September, there is a gradual displacement of the inner core of the high pressure to a more southerly position in the Atlantic margin of Europe, but, in conjunction, this high pressure region became more continuous over Southern Europe and the western Mediterranean. The persistence of the weak (thermal low) low over the IP (apparently with a broader influence over this region) is also noteworthy. For the period of 15–17 of September, there is a resurgence of the initial strength of the subtropical high (1033–1035 hPa). The eastern margin of this high pressure system is disturbed by a cold front associated with a frontal cyclone located over the British Islands, moving into the IP (15 of September). At the surface level immediately after the decay (18 of September), the influence of the subtropical high extended towards the western margin of Europe, while the cyclonic circulation associated with the weak low over Southern Spain and North of Africa remained active. Despite the synoptic chart limitations, mainly due to their coarse spatial resolution, they provide evidence for circulations favoring the occurrence of thunderstorms and lightning over Portugal during the selected episode.

As previously stated, a WRF run is carried out to simulate high-resolution atmospheric fields over Portugal during the current episode (the MERRA fields are defined on a much coarser grid; Table 1). Since a simulation covering the entire observational period of 2003–2009 is not currently available, the parameters simulated by WRF cannot yet be used in model fitting and estimation. As such, these fields are used here only for a better characterization of the dynamical features during this exceptional episode, leaving the full integration of the WRF in the statistical–dynamical modeling approach for an upcoming study. The composites of the WRF 700 hPa geopotential height and 10 m horizontal streamlines for the episode confirm the presence of a low pressure trough extending over southern Portugal, with a minimum core located southwestwards of Portugal and with strong wind confluence (Fig. 11). The secondary minimum over southern Portugal is still worth mentioning. The composites of the 500 hPa temperature and geopotential height underline the cut-off structure of this trough, with a cold core centered over southern-central Portugal, also indicating important baroclinicity and cyclogenesis.

All the dynamical conditions described above are particularly noticeable in the onset day (10.09.2007), which was also characterized by an explosive lightning activity (Fig. 11), particularly in the period 14–15:00 UTC, when the hourly maximum of CGD occurrences was recorded (1279 CGD h⁻¹). The low-tropospheric trough represented in the synoptic chart for this day (Fig. 10) is resolved in much greater detail by WRF (Fig. 11), but its axis is more southwest-northeastwardly tilted than can be inferred from the synoptic chart. The 10 m horizontal streamlines also reveal important flow confluentes all over the country, particularly over its southern half, which is an important tracer for the preferred locations of deep convective cells, also confirmed by the CGD pattern for that day (Fig. 9). Moreover, the mid-tropospheric cold core cut-off low is significantly enhanced and centered over southwestern Portugal, which is also in clear agreement with the location of the CGD over Portugal in this particular day (Fig. 9).

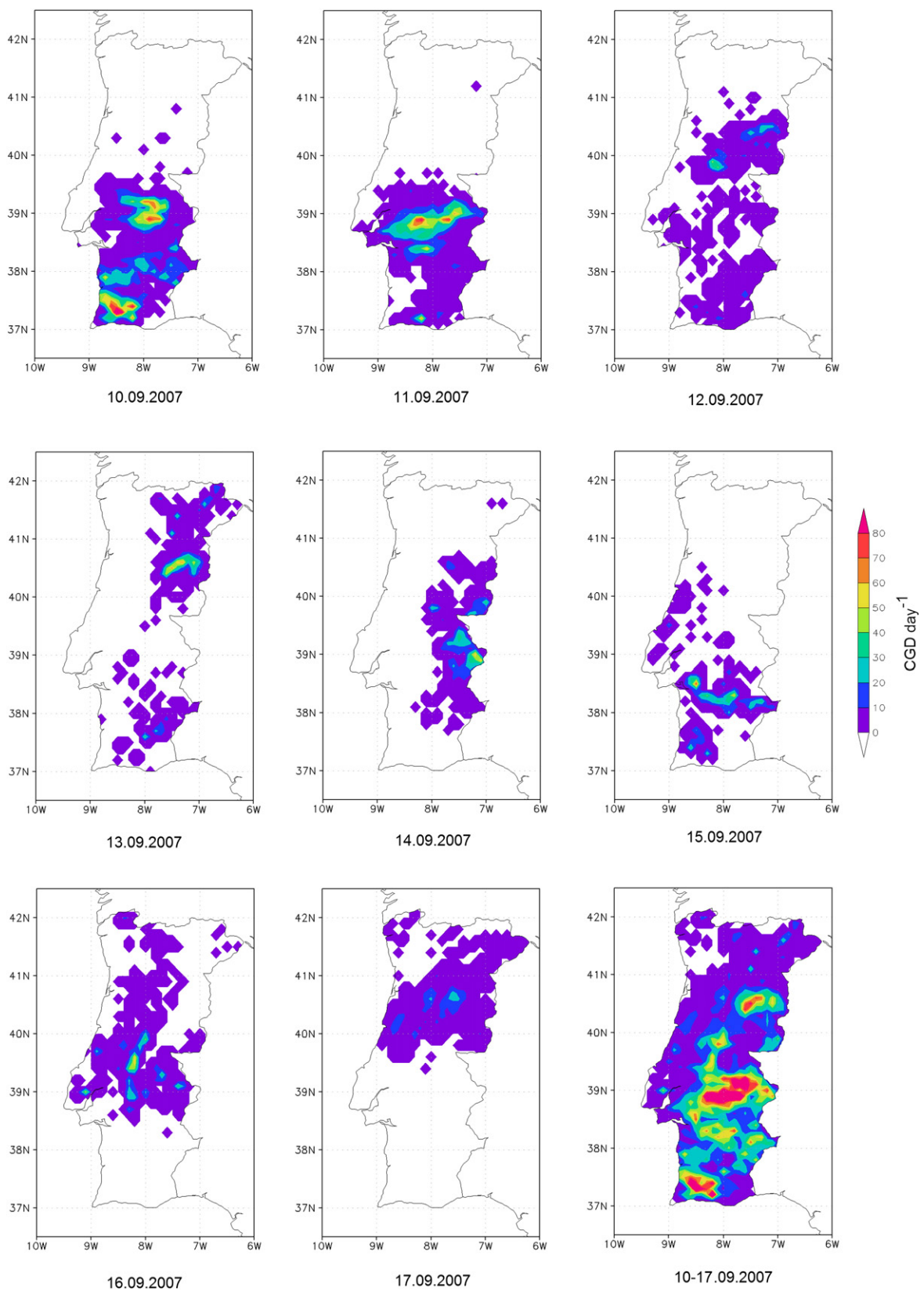


Fig. 9. Daily patterns of the CGD totals during the case study period (10–17 September 2007) and the corresponding sum over all days in this period (bottom left panel). A 0.5° latitude \times 0.5° longitude kernel smoothing was applied to the patterns.

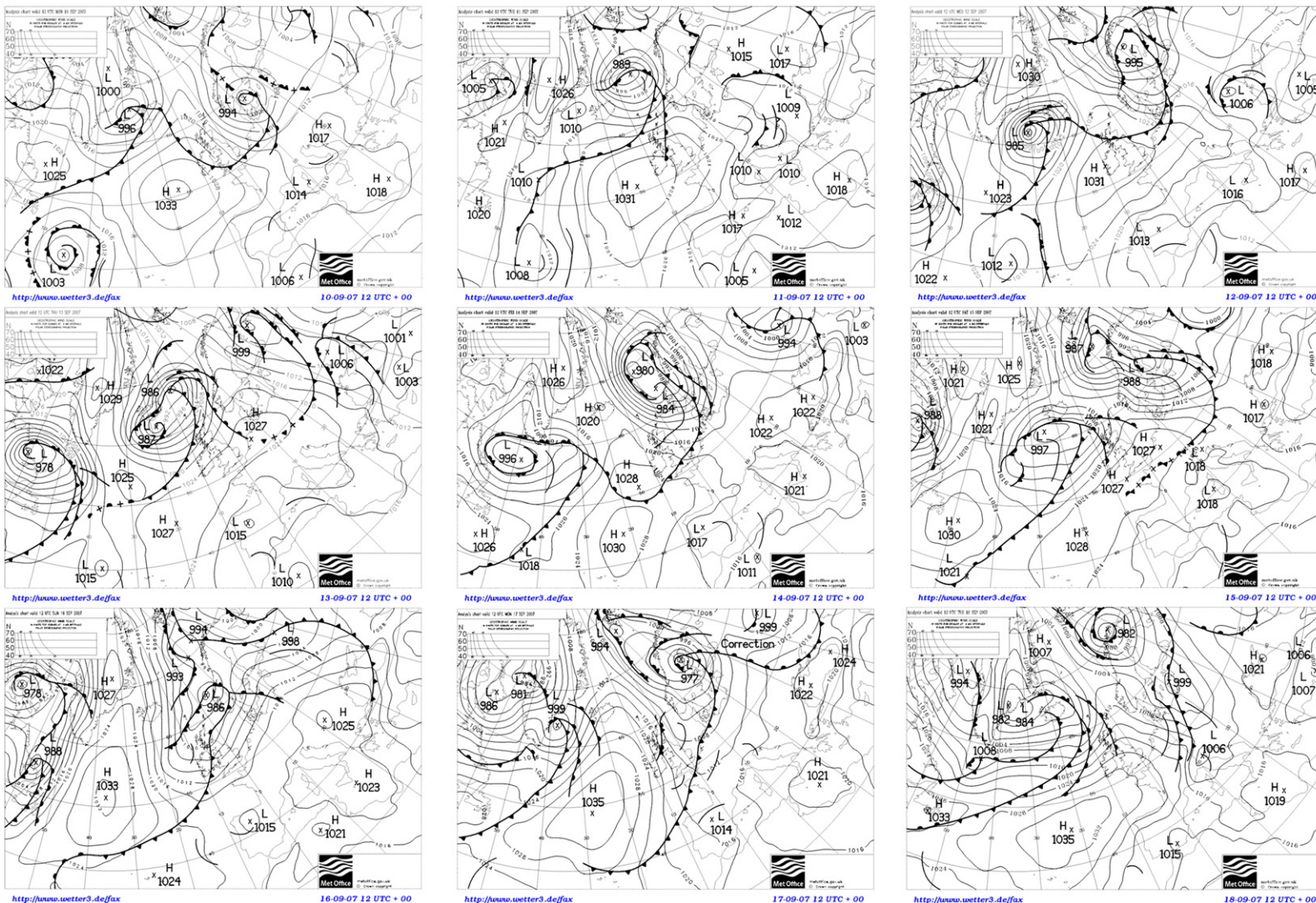


Fig. 10. Met Office synoptic charts during case study period (10–17 September 2007) and for one day after decay (18 September 2007).

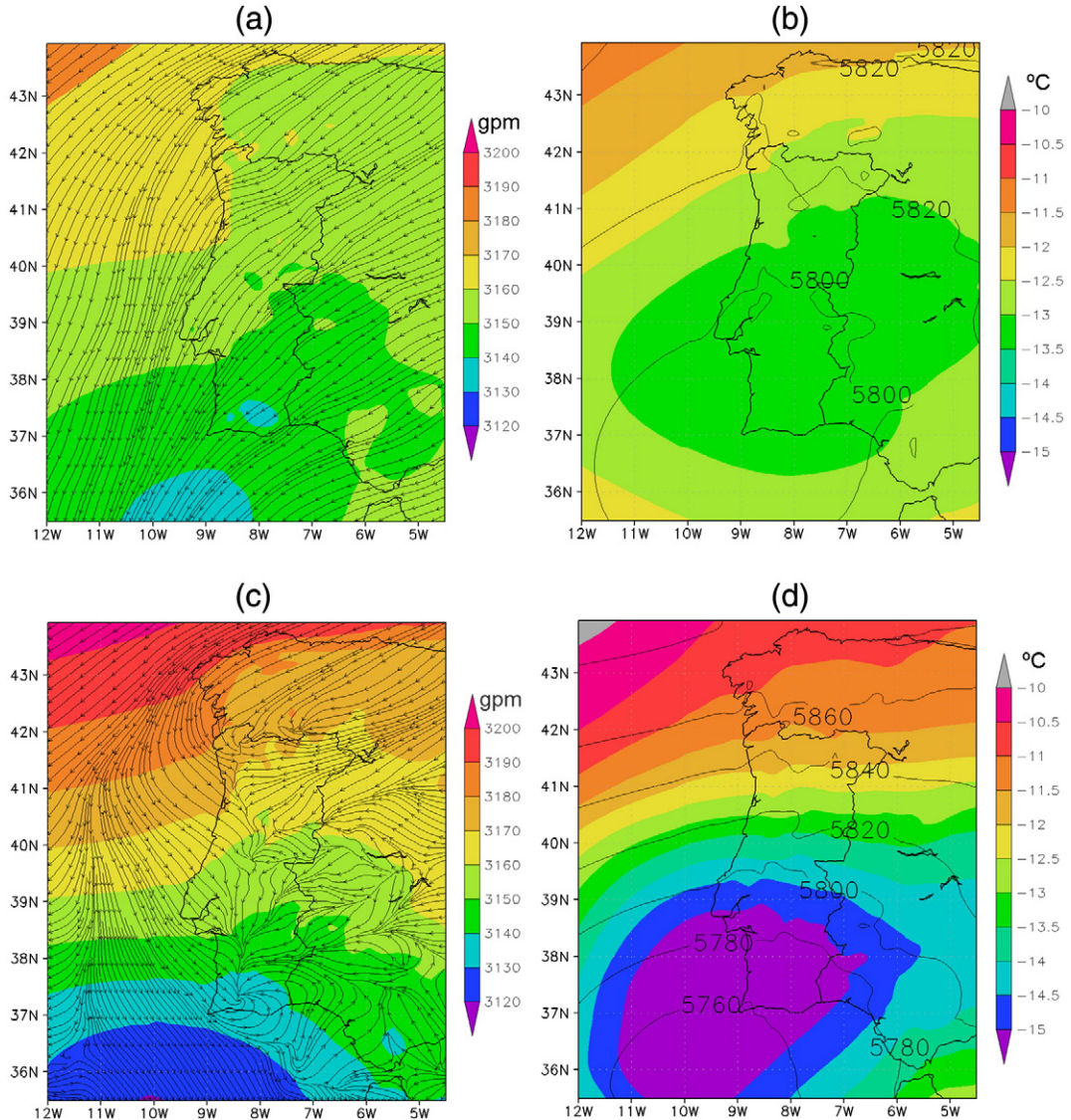


Fig. 11. Upper panels: Composites for the case study (10–17 September 2007) simulated by the WRF of the: (left) 700 hPa geopotential height (shading in gpm) and 10 m horizontal streamlines; (right) 500 hPa temperature (shading in °C) and geopotential height (contours in gpm). Lower panels: the same as in the upper panels, but the instantaneous fields in 10.09.2007 at 14:00 UTC (peak of CGD occurrences over the entire episode).

4. Summary and conclusions

Three lightning regimes are identified for Portugal (WREG, WREM and SREG) and their dynamical structure is characterized. The WREG is a typical cut-off low, with all its dynamical features coherent with a cold-core barotropic equivalent flow. Its intense cyclogenesis may trigger considerable lightning activity. The WREM is, in turn, linked to strong frontal systems, associated with remote low pressure systems at higher latitudes over the North Atlantic, which are embedded in a mid-tropospheric trough westwards of Portugal. The intense frontogenesis is clearly favorable to lightning activity. Lastly, the SREG is related to an inverted trough, extending from North Africa towards Portugal, and by a mid-tropospheric cold-core over Portugal. Both dynamical features simultaneously drive

very warm low-tropospheric temperatures and relatively cold mid-tropospheric temperatures, which generates strong vertical instability and stimulates deep convection and lightning activity.

Despite the large complexity of the physical mechanisms, the strength of the lightning activity (high and low activity classes) for each of these three regimes can be reliably modeled by some suitable dynamical predictors, with global efficiencies ranging from 65 to 70%. The difference of the equivalent potential temperature in the 700–500 hPa layer emerges as the best predictor for the three regimes. In fact, this measure is equivalent to a static stability index for a saturated air parcel in a layer, determinant for the development of deep convective cells and thunderstorms. The best 4-layer lifted index also shows to be a significant dynamical predictor for the three regimes, but the relationships are

much weaker. Other predictors are more suitable for a given regime, namely the 500 hPa potential vorticity for the WREG, the difference of the relative humidity in 700–500 hPa and the moist static stability index at 700 hPa for the WREM, the 300 hPa equivalent potential temperature, the 700 hPa potential vorticity and the difference of the specific humidity in 700–500 hPa for the SREG.

A statistical-dynamical modeling of the daily CGD occurrences is developed by using logistic regression models (statistical component) for each regime separately (dynamical component). The skill of this modeling is also demonstrated for the episode with the strongest ever recorded lightning activity in Portugal (10–17 September 2007). A WRF simulation is used for a better description of the atmospheric fields. In future research, however, we also aim to use WRF simulated predictors to improve this statistical-dynamical modeling approach. Up to now and outside Portugal, some studies have been carried out in order to investigate the skill of the WRF model to forecast the occurrence of lightning flashes, by developing and testing methods to estimate flash densities, flash rates or its incidence over a region (e.g. and respectively, McCaul et al., 2009; Barthe et al., 2010; Zepka et al., 2013). A comparative analysis of the lightning forecasts in Portugal using both the present study logistic models and the WRF will be carried out in a forthcoming study.

As our statistical-dynamical approach for daily CGD modeling provides valuable information regarding the expected strength of the lightning activity over Portugal, it might be particularly relevant in operational weather forecasting. This ability can represent a breakthrough in the application of the forecasts to many socioeconomic activities. In addition to the numerous studies devoted to lightning or thunderstorm prediction within operational meteorology (as cited in Section 1), the utility of lightning prediction models have also been suggested with regard to other applications, like wildfire weather forecasting (Peterson and Wang, 2010). Further, lightning often causes damages on the electric power network, wind power plants (e.g. Rodrigues et al., 2011) and industrial facilities (Renni et al., 2010), which are commonly cataloged as natural disasters. Hence, lightning forecasts can have beneficial effects on electric power production, distribution and network planning.

Local (grid point) modeling was also tested, but the relationships were much weaker and the model skills very poor. In fact, the point-by-point correlations between CGD occurrences/classes and the atmospheric parameters used in the present study revealed a high spatial and seasonal inconsistency. Underlying this difficulty might be the key role played by local surface conditions, such as those related to orography, soils and microclimatic features, in directing the precise location of the convective cells and of the associated lightning activity. Therefore, it can be concluded that modeling daily CGD totals within geographical sectors is preferable over grid point modeling. An attempt to model daily CGD within subsectors in Portugal will be developed in a forthcoming study.

Acknowledgments

The present research was undertaken within the project “Lightning activity in Portugal: variability patterns and socio-economic impacts (RAIDEN)”, funded by the Fundação para a

Ciência e a Tecnologia (FCT), under the contract number PTDC/CTE-ATM/101931/2008. This work is also supported by the European Union Funds (FEDER/COMPETE—Operational Competitiveness Programme) and by the national funds (FCT)—under the project FCOMP-01-0124-FEDER-022692. We would like to acknowledge the Instituto Português do Mar e da Atmosfera (IPMA), for providing the CGD dataset. MERRA data used in this effort were acquired as part of the activities of NASA's Science Mission Directorate, and are archived and distributed by the Goddard Earth Sciences (GES) Data and Information Services Center (DISC). We acknowledge the Japan Meteorological Agency (JMA)—Central Research Institute of Electric Power Industry (CRIEPI) for supplying their reanalysis data, and the University Corporation for Atmospheric Research (UCAR), for providing their best 4-layer lifted index.

References

- Almeida, S., Loureiro, C., Barbosa, F., Pestana, R., 2009. Historical data analysis of lightning and its relation with the Portuguese transmission system outages. IEEE Bucharest Power Tech Conference, June 28th–July 2nd, Bucharest, Romania.
- Altaratz, O., Levin, Z., Yair, Y., Ziv, B., 2003. Lightning activity over land and sea on the Eastern Coast of the Mediterranean. *Mon. Weather Rev.* 131, 2060–2070.
- Areatio, J., Ezcurrea, A., Herrero, I., 2001. Cloud-to-ground lightning characteristics in the Spanish Basque Country area during the period 1992–1996. *J. Atmos. Sol. Terr. Phys.* 63 (10), 1005–1015.
- Barthe, C., Deierling, W., Barth, M.C., 2010. Estimation of total lightning from various storm parameters: a cloud resolving model study. *J. Geophys. Res.* 115, D24202.
- Belsley, D.A., Kuh, E., Welsh, R.E., 1980. *Regression Diagnostics*. John Wiley & Sons, Inc., New York, NY.
- Burrows, H.R., Price, C., Wilson, L.J., 2005. Warm season lightning probability prediction for Canada and the Northern United States. *Weather. Forecast.* 20, 971–988.
- Carvalho, R., Prior, V., Deus, R., 2003. Exploração experimental do sistema rede de detectores de trovoadas. 3º Simpósio de Meteorologia e Geofísica da APMG, 4º Encontro Luso-Espanhol de Meteorologia, Aveiro, Portugal, 10–13 February 2003, p. 36.
- Chen, F., Dudhia, J., 2001. Coupling an advanced land-surface/hydrology model with the Penn State/NCAR MM5 modeling system. Part I: model description and implementation. *Mon. Weather Rev.* 129, 569–585.
- Christian, H.J., Blakeslee, R.J., Goodman, S.J., Mach, D.A., Stewart, M.F., Buechler, D.E., Koshak, W.J., Hall, J.M., Boeck, W.L., Driscoll, K.T., Boccippio, D.J., 1999. The lightning imaging sensor. Proceedings of the 11th International Conference on Atmospheric Electricity, Guntersville, Alabama, June 7–11, pp. 746–749.
- Cummins, K., Murphy, M., 2009. An overview of lightning locating systems: history, techniques and data uses with an in-depth look at the U.S. NLDN. *IEEE Trans. Electromagn. Compat.* 51, 499–518.
- Curran, E., Holle, R., López, R., 2000. Lightning casualties and damages in the United States from 1959 to 1994. *J. Clim.* 13, 3448–3464.
- De Pablo, F., Rivas-Soriano, L., 2007. Winter lightning and North Atlantic Oscillation. *Mon. Weather Rev.* 135, 2810–2815.
- Defer, E., Lagouvardos, K., Kotroni, V., 2005. Lightning activity in the eastern Mediterranean region. *J. Geophys. Res.* 110, D24210. <http://dx.doi.org/10.1029/2004JD005710>.
- García-Ortega, E., Trobajo, M.T., López, L., Sánchez, J.L., 2011. Synoptic patterns associated with wildfires caused by lightning in Castile and Leon, Spain. *Nat. Hazards Earth Syst. Sci.* 11, 851–863.
- Grell, G.A., Devenyi, D., 2002. A generalized approach to parameterizing convection combining ensemble and data assimilation techniques. *Geophys. Res. Lett.* 29 (14) (Article 1693).
- Haklander, A.J., Van Delden, A., 2003. Thunderstorm predictors and their forecast skill for the Netherlands. *Atmos. Res.* 67–68, 273–299.
- Hong, S.-Y., Lim, J.-O., 2006. The WRF Single-Moment 6-Class Microphysics Scheme (WSM6). *J. Korean Meteor. Soc.* 42, 129–151.
- Hong, S.-Y., Noh, Y., Dudhia, J., 2006. A new vertical diffusion package with an explicit treatment of entrainment processes. *Mon. Weather Rev.* 134, 2318–2341.
- Janjic, Z.I., 2002. Nonsingular Implementation of the Mellor-Yamada Level 2.5 Scheme in the NCEP Meso Model. NCEP Office Note, No. 437 (61 pp.).

- Librantz, H., Librantz, A., 2006. Descargas elétricas atmosféricas e suas interações com aeronaves. *Exacta* 4 (002), 247–258.
- Lynn, B., Yair, Y., 2010. Prediction of lightning flash density with the WRF model. *Adv. Geosci.* 23, 11–16.
- Mazany, R.A., Gutman, S.I., Roeder, W., 2002. A lightning prediction index that utilizes GPS integrated precipitable water vapor. *Weather. Forecast.* 17, 1034–1047.
- McCaull, E.W., Goodman, S.J., Lacasse, K.M., Cecil, D.J., 2009. Forecasting lightning threat using cloud-resolving model simulations. *Weather. Forecast.* 24, 709–729.
- Mills, B., Unruh, D., Pentelow, L., Spring, K., 2010. Assessment of lightning-related damage and disruption in Canada. *Nat. Hazards* 52, 481–499.
- Morrison, H., Thompson, G., Tatarki, V., 2009. Impact of cloud microphysics on the development of trailing stratiform precipitation in a simulated squall line: comparison of one- and two-moment schemes. *Mon. Weather Rev.* 137, 991–1007.
- Onogi, K., Tsutsui, J., Koide, H., Sakamoto, M., Kobayashi, S., Hatushika, H., Matsumoto, T., Yamazaki, N., Kamahori, H., Takahashi, K., Kadokura, S., Wada, K., Kato, K., Oyama, R., Ose, T., Manojoji, N., Taira, R., 2007. The JRA-25 reanalysis. *J. Meteorol. Soc. Jpn.* 85, 369–432.
- Peterson, D., Wang, J., 2010. Effects of lightning and other meteorological factors on fire activity in the North American boreal forest: implications for fire weather forecasting. *Atmos. Chem. Phys.* 10, 6873–6888.
- Ramos, R., Prior, V., Correia, S., Deus, R., 2007. Portuguese lightning detection network (2003–2006). Second International Symposium on Lightning Physics and Effects European COST Action P18 (available at: http://www.costp18-lightning.org/Publications/symposium2007/5_8_Ramos.pdf (accessed in the 23th November 2012)).
- Ramos, A.M., Ramos, R., Sousa, P., Trigo, R.M., Janeira, M., Prior, V., 2011. Cloud to ground lightning activity over Portugal and its association with circulation weather types. *Atmos. Res.* 101 (1–2), 84–101.
- Renni, E., Krausmann, E., Cozzani, V., 2010. Industrial accidents triggered by lightning. *J. Hazard. Mater.* 184 (1–3), 42–48.
- Rienecker, M.M., Suarez, M.J., Gelaro, R., Todling, R., Bacmeister, J., Liu, E., Bosilovich, M.G., Schubert, S.D., Takacs, L., Kim, G.-K., Bloom, S., Chen, J., Collins, D., Conaty, A., da Silva, A., Gu, W., Joiner, J., Koster, R.D., Lucchesi, R., Molod, A., Owens, T., Pawson, S., Piegion, P., Redder, C.R., Reichle, R., Robertson, F.R., Ruddick, A.G., Sienkiewicz, M., Woollen, J., 2011. MERRA: NASA's modern-era retrospective analysis for research and applications. *J. Clim.* 24 (14), 3624–3648. <http://dx.doi.org/10.1175/jcli-d-11-00015.1>.
- Rivas-Soriano, L., De Pablo, F., 2002. Effect of small urban areas in central Spain on the enhancement of cloud-to-ground lightning activity. *Atmos. Environ.* 36, 2809–2816.
- Rivas-Soriano, L., De Pablo, F., Diez, E., 2001. Cloud-to-ground lightning activity in the Iberian Peninsula: 1992–1994. *J. Geophys. Res.* 106 (11), 891–901.
- Rivas-Soriano, L., De Pablo, F., Diez, E., 2001. Relationship between convective precipitation and cloud-to-ground flashes in the Iberian Peninsula. *Mon. Weather Rev.* 129, 2998–3003.
- Rivas-Soriano, L., De Pablo, F., Diez, E., 2001. Meteorological and geographical relationships with lightning activity in Castilla-Leon (Spain). *Meteorol. Appl.* 8, 169–175.
- Rivas-Soriano, L., De Pablo, F., Tomás, C., 2004. Impact of the North Atlantic Oscillation on winter convection: convective precipitation and cloud-to-ground lightning. *Int. J. Climatol.* 24, 1241–1247.
- Rivas-Soriano, L., De Pablo, F., Tomás, C., 2005. Ten-year study of cloud-to-ground lightning activity in the Iberian Peninsula. *J. Atmos. Sol. Terr. Phys.* 67, 1632–1639.
- Rodrigues, R., Mendes, V., Catalão, J., Correia, S., Prior, V., Aguado, M., 2009. Analysis of the thunderstorm activity in Portugal for its application in the lightning protection of wind turbine. *IEEE Lat. Am. Trans.* 7 (5), 519–526.
- Rodrigues, R., Mendes, V., Catalão, J., 2010. Lightning data observed with lightning location system in Portugal. *IEEE Trans. Power Delivery* 25 (2), 870–875.
- Rodrigues, R., Mendes, V., Catalão, J., 2011. Protection of wind energy systems against the indirect effects of lightning. *Renew. Energy* 36 (11), 2888–2896.
- Rorig, M., Ferguson, S., 1999. Characteristics of lightning and wildland fire ignition in the Pacific northwest. *J. Appl. Meteorol.* 38, 1565–1575.
- Sánchez, J.L., García-Ortega, E., Marcos, J.L., 2001. Construction and assessment of a logistic regression model to short-term forecasting of thunderstorms in León (Spain). *Atmos. Res.* 56, 57–71.
- Sánchez, J.L., Marcos, J.L., Dessens, J., López, L., Bustos, C., García-Ortega, E., 2008. Assessing sounding-derived parameters as storm predictors in different latitudes. *Atmos. Res.* 56, 57–71.
- Sánchez, J.L., López, L., Bustos, C., Marcos, J.L., García-Ortega, E., 2008. Short-term forecast of thunderstorms in Argentina. *Atmos. Res.* 88, 36–45.
- Santos, J., Reis, M., Sousa, J., Leite, S., Correia, S., Janeira, M., Fragoso, M., 2012. Cloud-to-ground lightning in Portugal: patterns and dynamical forcing. *Nat. Hazards Earth Syst. Sci.* 12, 639–649.
- Shafer, P.E., Fuelberg, H.E., 2006. A statistical procedure to forecast warm season lightning over portions of the Florida Peninsula. *Weather. Forecast.* 21, 851–869.
- Shalev, S., Saaroni, H., Izsak, T., Yair, Y., Ziv, B., 2011. The spatio-temporal distribution of lightning over Israel and the neighboring area and its relation to regional synoptic systems. *Nat. Hazards Earth Syst. Sci.* 11, 2125–2135. <http://dx.doi.org/10.5194/nhess-11-2125-2011>.
- Skamarock, W.C., Klemp, J.B., 2007. A time-split nonhydrostatic atmospheric model for research and NWP applications. *J. Comput. Phys.* 3465–3485 (Special issue on environmental modeling).
- Skamarock, W.C., Klemp, J.B., Dudhia, J., Gill, D.O., Barker, D.M., Duda, M.G., Huang, X.Y., Wang, W., Powers, J.G., 2008. A description of the Advanced Research WRF Version 3. NCAR Tech. Notes.
- Soares, P., Cardoso, R., Miranda, P., Medeiros, J., Belo-Pereira, M., Espírito-Santo, F., 2012. WRF high resolution dynamical downscaling of ERA-Interim for Portugal. *Clim. Dyn.* 39 (9–10), 2497–2522.
- Trigo, R.M., DaCamara, C.C., 2000. Circulation weather types and their influence on the precipitation regime in Portugal. *Int. J. Climatol.* 20, 1559–1581.
- Wilks, D.S., 2006. Statistical Methods in the Atmospheric Sciences. Academic Press, USA.
- Yair, Y., Lynn, B., Price, C., Kotroni, V., Lagouvardos, K., Morin, E., Mugnai, A., Llasat, M.C., 2010. Predicting lightning density in Mediterranean storms based on the WRF model dynamic and microphysical fields. *J. Geophys. Res.* 115, D04205. <http://dx.doi.org/10.1029/2008JD010868>.
- Zepka, G.S., Pinto Jr., O., Saraiva, A.C.V., 2012. Influence of initial conditions on lightning forecasting using the WRF model. 22nd International Lightning Detection Conference and 4th International Lightning Meteorology Conference, Broomfield, Colorado, USA.
- Zepka, G.S., Pinto Jr., O., Saraiva, A.C.V., 2013. Lightning forecasting in southeastern Brazil using the WRF model. *Atmos. Res.* <http://dx.doi.org/10.1016/j.atmosres.2013.01.008>.
- Ziv, B., Saaroni, H., Yair, Y., Ganot, M., Baharad, A., Isaschari, D., 2009. Atmospheric factors governing winter thunderstorms in the coastal region of the eastern Mediterranean. *Theor. Appl. Climatol.* 95, 301–310.

Glossary

- PV_{500} : Maximum potential vorticity at 500 hPa
- PV_{700} : Maximum potential vorticity at 700 hPa
- SSI_{700} : Minimum static stability index at 700 hPa
- θ_{eq300} : 300 hPa equivalent potential temperature
- $\Delta d_{700 - 500}$: 700–500 hPa differences in the specific humidity
- $\Delta RH_{700 - 500}$: 700–500 hPa differences in the relative humidity
- $\Delta \theta_{eq700 - 500}$: 700–500 hPa differences in the equivalent potential temperature
- AEMET: Agência Estatal de Meteorologia (Spain)
- CGD: Cloud-to-Ground Discharges
- CREPI: Central Research Institute of Electric Power Industry
- DISC: Data and Information Services Center
- GDAS: Global Data Assimilation System
- GES: NASA Goddard Earth Sciences
- HGT: Geopotential height
- IP: Iberian Peninsula
- IPMA: Instituto Português do Mar e da Atmosfera
- JMA: Japan Meteorological Agency
- JRA: Japanese Reanalysis Dataset
- LCGD: Log-transformed CGD
- LDN: Lightning Detection Network
- LI: Best 4-layer Lifted Index
- MDISC: Modelling and Assimilation Data and Information Services Center
- MERRA: Modern Era Retrospective-analysis for Research and Applications
- MSLP: Mean Sea Level Pressure
- NAO: North Atlantic Oscillation
- NCEP FNL: National Centers for Environmental Prediction Final
- P50: Median distribution
- PC: Principal Components
- PS: Portuguese sector
- PV: Potential vorticity
- q: Specific humidity
- RH: Relative humidity
- SREG: Summer regional regime
- SRM: Shuttle Radar Topography Mission
- SSI: Static Stability Index
- T: Air temperature
- U: Zonal wind component
- UCAR: University Corporation for Atmospheric Research
- V: Meridional wind component
- WREG: Winter regional regime
- WREM: Winter remote regime
- WRF: Weather Research and Forecasting



João F. Sousa is Meteorologist in the Portuguese Meteorological Office since 1993. He is a PhD student in Physical Sciences at the University of Trás-os-Montes e Alto-Douro (UTAD). He holds a MSc in Climate and Climatic Change at the UTAD in 2009. He is Member of the Centre for Research and Technology of Agro-Environmental and Biological Sciences (CITAB). His main research interests are atmospheric dynamics and climate variability.



João Corte-Real is Emeritus Professor at the University of Évora, Portugal. Currently, he is researcher at the Institute of Mediterranean Agricultural and Environmental Sciences (ICAAM) and coordinator of the group "Water, Soil and Climate" (since 2007). He was also Professor at the Faculty of Sciences of the University of Lisbon (FCUL) for 38 years. In 1991, he created the group of Meteorology/Climatology of the Physics Department/Institute of Applied Science and Technology (ICAT) at the FCUL for research in climate dynamics, statistical climatology, climate variability, climate change impacts and numerical simulation of the atmospheric circulation on a regional scale. He was supervisor of more than one hundred students at all levels and participated in hundreds of national/international projects.



Marcelo Fragoso is currently Assistant Professor of IGOT-UL (Institute of Geography and Spatial Planning, University of Lisbon) since 2004. He holds a PhD in Physical and Regional Geography, University of Lisbon, 2004. He is Researcher of the Centre for Geographical Studies (IGOT-UL) with affiliation as team member of the research groups CliMA—Climate and Environmental Changes (principal affiliation) and RISKam—Environmental Hazards and Risk Assessment and Management (secondary affiliation). Currently, he is coordinator of the research project "Raiden" (2010–2013) and member of the

research projects "Disaster" (2010–2013) and "KlimHist" (2010–2013). His main research interests are Climate Variability, Hydroclimatology, Applied Climatology, Extreme Weather and Climate Events.



João A. Santos is currently Professor at the Physics Department of the University of Trás-os-Montes e Alto Douro (UTAD), Vila Real, Portugal. Academic degrees: Aggregation in Physics at the UTAD in 2012; PhD in Climatology/Meteorology at the University of Lisbon in 2005; MSc at the UTAD in 1999; Graduation in Physics/Geophysics at the University of Lisbon in 1995. Area of research: Atmospheric and Environmental Sciences. Current R&D Centre: Centre for the Research and Technology of Agro-Environmental and Biological Sciences. Projects: Member of 15 research projects, 5 of them international (2 EU funded projects). Authorship: 24 JCR-indexed papers, 11 books/book chapters and over than 150 publications/proceedings in scientific meetings and seminars. Teaching experience: over than 40 curricular units or specialized courses. Supervision: 26 PhD or MSc students.



Currently **Susana Mendes** is currently a post-doctoral fellow at the Geophysical Institute of the University of Bergen, Norway. She holds a PhD in Physics-Meteorology from the University of Aveiro, Portugal, 2011. She was a visiting scientist at the Department of Atmospheric Sciences of University of Washington, USA, from 2006 to 2009. Scientific collaboration in MICE and PRUDENCE European projects, as well as, CAPEX/CLAPREC observational campaign and RAIDEN project, both focused in understanding deep convection over Portugal. Her main research interests are cloud physics and dynamics and cloud processes modeling, tropical deep convection and ocean-atmosphere interaction and its relation to climate.